

Anomalous magnetic response of the spin-one-half Falicov-Kimball model

J. K. Freericks and V. Zlatić[†]

Department of Physics, Georgetown University, Washington, DC 20057

(June 24, 2018)

Abstract

The infinite-dimensional spin one-half Falicov-Kimball model in an external magnetic field is solved exactly. We calculate the magnetic susceptibility in zero field, and the magnetization as a function of the field strength. The model shows an anomalous magnetic response from thermally excited local moments that disappear as the temperature is lowered. We describe possible real materials that may exhibit this kind of anomalous behavior.

I. INTRODUCTION

The spin-one-half Falicov-Kimball model¹ was introduced in 1969 to describe metal-insulator transitions in transition-metal and rare-earth compounds. The metal-insulator transition is a charge-transfer transition, where the system consists of both localized (insulating) electronic states and delocalized (conducting) electronic states, and the transition occurs when the electron filling switches from the localized to delocalized states (or vice versa). This is the simplest possible metal-insulator transition, since the character of the individual electronic states does not change at the transition, rather it is just the occupancy of those states that varies.

The localized electrons are strongly interacting with each other, so double occupancy of the localized orbitals is forbidden. The conduction electrons, however, are chosen to be noninteracting, since the Coulomb interaction between them is screened. The only remaining interaction term in the Falicov-Kimball model is the mutual repulsion between a conduction and localized electron that sit on the same lattice site. For any fixed configuration of the localized electrons, the quantum-mechanical problem for the conduction electrons can be solved in a single-particle basis. The many-body aspects enter from taking an annealed thermal average over all possible configurations of the localized electrons.

We are most interested in the situation where the localized level lies just above the Fermi energy, so there are no localized electrons at $T = 0$. As the temperature rises, then it becomes more favorable to thermally occupy the localized levels because of the gain in entropy of the local moments. This will have a dramatic effect on the uniform spin susceptibility, as the localized electrons will generate a Curie-like response, which is much larger than the Pauli-like response of the conduction electrons. The net effect is that the susceptibility will show a peak at a characteristic temperature which is determined by the point where the localized electron occupancy saturates. In addition, we expect there to be interesting behavior as a function of magnetic field, where the proximity of the localized levels close to the Fermi energy can induce a rapid change in the magnetization, producing metamagnetism.

The Falicov-Kimball model was initially applied to a wide variety of transition-metal and rare-earth compounds such as SmB_6 , V_2O_3 , NiS , etc. which display both continuous and discontinuous metal-insulator transitions as a function of either temperature or pressure. However, the Falicov-Kimball model has not been generally accepted as explaining the metal-insulator transitions of all of these different materials for two reasons. First, it neglects all effects of hybridization, and hence all Kondo-effect physics, and second it does not take into account the fact that most of these materials also undergo a structural phase transition.

Recently, however, a new material was discovered that undergoes a classic charge-transfer metal-insulator transition without any structural phase transition—it is NiI_2 when put under high pressure². This layered compound crystallizes in the CdCl_2 crystal structure, in which the Ni ions form a close-packed plane, with close-packed I planes lying both above and below. The NiI_2 planes are then stacked in an alternating packing scheme. The Fermi level of NiI_2 lies within the Ni d-bands, since the Ni donates one electron to each I ion that lies in

© 1998 by the authors. Reproduction of this article by any means is permitted for non-commercial purposes.

the plane above and below. The ground state is an antiferromagnetic insulator. As pressure is applied, the I p-bands move closer to the Fermi level causing the Néel temperature to rise, until they reach the Fermi level, and electrons from the I ions move onto the Ni^{++} ions changing them to Ni^+ and quenching the local magnetic moment. The remaining holes in the I p-bands are conducting, and the material becomes metallic.

Another class of materials that might be described by an effective Falicov-Kimball model is the class of Yb-based valence-fluctuating (VF) compounds (like YbInCu_4 , $\text{YbIn}_{1-x}\text{Ag}_x\text{Cu}_4$ and $\text{Yb}_{1-x}\text{Y}_x\text{InCu}_4$) which exhibit large anomalies in their thermodynamic³⁻⁵, spectroscopic^{3,6,7} and transport properties^{3,5,8}, around a characteristic, sample-dependent temperature T_V (40 – 60K). The magnetic susceptibility $\chi(T)$ of these compounds is of a Curie-Weiss form at high temperatures, and the anomaly appears^{5,8,9}, as a pronounced asymmetric peak just above this characteristic sample-dependent temperature T_V . Below T_V , $\chi(T)$ exhibits Pauli-like behavior, while at the lowest temperatures a weak Curie-like upturn is often seen. The X-ray analysis shows that the Yb-based VF compounds crystallize in a C15b structure, that the lattice constant $a(T)$ changes at T_V by a small amount^{6,8,10}, and that there are no structural changes. There is no evidence^{4,6} for magnetic ordering below T_V , instead the Yb ions fluctuate between a 2+ and 3+ state, but the average volume change at T_V is much less than what one would expect from a complete Yb^{3+} - Yb^{2+} transition.³ The anomaly in the high-field magnetization of YbInCu_4 ⁴ and $\text{YbIn}_{1-x}\text{Ag}_x\text{Cu}_4$ ¹¹ appears as a sudden increase of the slope and the saturation of $M(H)$ at about $H_V \simeq 30 - 50 T$. The Zeeman energy at H_V (at $T \ll T_V$) is comparable to the thermal energy at T_V (at $H \ll H_V$). At elevated temperatures, this metamagnetic transition disappears⁶. The magnetostriction data⁴ indicate that the metamagnetism relates to the valence fluctuations of the Yb ions but the field-induced change of the f -electron valence is even smaller than the temperature-induced one.

The large magnetic anomalies accompanied by small lattice changes can be reconciled by a model in which there is some intrinsic disorder between Yb and In sites, such that a minority of Yb ions (in the C15b lattice) lie at “ill-placed sites”. The correctly placed Yb ions are hybridized with the ligands and are in the VF state at all temperatures. The “ill-placed” Yb ions are unhybridized (because the Yb-In distance of an “ill-placed” Yb ion [that sits on an In site] is nearly twice as large as the Yb-In distance for an Yb ion that sits on the correct lattice site) and undergo a charge-transfer transition at T_V (one 4f electron jumps into conduction band and leaves behind a magnetic hole). As a consequence, the susceptibility acquires a large asymmetric peak just above T_V , while the low-temperature magnetization exhibits a metamagnetic transition for magnetic fields of the order of $k_B T_V$.

This recent experimental work provides our motivation to study the magnetic response of the spin-one-half Falicov-Kimball model, and to compare the results with the available susceptibility data for NiI_2 and YbInCu_4 . On the theoretical side, the Falicov-Kimball model has also received renewed interest, with work concentrating on the linear and nonlinear characteristics of the model¹² and on the intermediate-valence and metal-insulator transitions¹³.

In Section II we present the formalism, showing how to determine the Green’s functions in a magnetic field, and the different magnetic and charge-density-wave response functions in zero field, and the numerical methods employed in the exact solution of the problem. Section III presents our results for the infinite-dimensional hypercubic lattice and Section IV summarizes the possible applications to real materials. Our conclusions appear in Section

V.

II. FORMALISM

The Hamiltonian of the Falicov-Kimball model consists of two types of spin-one-half electrons: conduction electrons (created or destroyed at site i by $d_{i\sigma}^\dagger$ or $d_{i\sigma}$) and localized electrons (created or destroyed at site i by $f_{i\sigma}^\dagger$ or $f_{i\sigma}$). The conduction electrons can hop between nearest-neighbor sites, with a hopping matrix $-t_{ij} =: -t^*/2\sqrt{D}$, where we have chosen to examine hypercubic lattices in D -dimensions, and we choose a scaling of the hopping matrix that yields a nontrivial limit in infinite-dimensions ($D \rightarrow \infty$)¹⁴. The f -electrons have a site energy E_f (which will be chosen to lie just above the Fermi energy at $T = 0$), and a chemical potential μ is employed to conserve the total number of electrons $n_{d\uparrow} + n_{d\downarrow} + n_{f\uparrow} + n_{f\downarrow} = \text{constant}$. Finally, there is a restriction of no double occupancy of the f -electrons on any site (implying the Coulomb repulsion U_{ff} between two f -electrons is infinite) and there is a Coulomb interaction U between the d - and f -electrons that occupy the same lattice site. In addition, we include a coupling to an external magnetic field h with a Landé g -factor added for the localized electrons. The resulting Hamiltonian is^{1,15}

$$\begin{aligned}
H = & \sum_{ij,\sigma} (-t_{ij} - \mu\delta_{ij}) d_{i\sigma}^\dagger d_{j\sigma} + \sum_{i,\sigma} (E_f - \mu) f_{i\sigma}^\dagger f_{i\sigma} \\
& + U \sum_{i,\sigma\sigma'} d_{i\sigma}^\dagger d_{i\sigma} f_{i\sigma'}^\dagger f_{i\sigma'} + U_{ff} \sum_{i,\sigma} f_{i\uparrow}^\dagger f_{i\uparrow} f_{i\downarrow}^\dagger f_{i\downarrow} \\
& - \mu_B h \sum_{i,\sigma} \sigma (2d_{i\sigma}^\dagger d_{i\sigma} + g f_{i\sigma}^\dagger f_{i\sigma}).
\end{aligned} \tag{1}$$

We solve the Falicov-Kimball model by working in the infinite-dimensional limit. The bare density of states $\rho(\epsilon)$ on a hypercubic lattice becomes

$$\rho(\epsilon) = \frac{1}{\sqrt{\pi t^*}} \exp[-\epsilon^2/t^{*2}], \tag{2}$$

and we take t^* as the unit of energy ($t^* = 1$). (The alternative lattice to consider is the Bethe lattice, where the bare density of states becomes Wigner's semicircle. The latter density of states is closer to a three-dimensional band because it increases like \sqrt{E} at the band edges. Since the Fermi level always lies far away from the band edge in all calculations considered here, we don't expect there to be much difference between the solution on a Bethe lattice versus on a hypercubic lattice. In fact, we have checked that this is not the case for our results in Section III.) In the infinite-dimensional limit the local approximation becomes exact¹⁴ so that the self energy has no momentum dependence, and the local conduction-electron Green's function satisfies

$$G_\sigma(i\omega_n) =: G_{n\sigma} = \int \frac{\rho(\epsilon)}{i\omega_n + \mu - \Sigma_{n\sigma} - \epsilon} d\epsilon, \tag{3}$$

where $\omega_n =: \pi T(2n+1)$ is the Fermionic Matsubara frequency, and $\rho(\epsilon)$ is the noninteracting density of states. The self-energy is determined by a three-step process: (i) first, the site-excluded Green's function $G_\sigma^0(i\omega_n)$, which holds the information about all of the other lattice sites, is found by adding back the self energy,

$$G_{\sigma}^0(i\omega_n) = \frac{1}{G_{n\sigma}^{-1} + \Sigma_{n\sigma}}; \quad (4)$$

then (ii) the local Green's function is calculated from a weighted sum over the different possible localized-electron states,

$$G_{n\sigma} = w_0 G_{\sigma}^0(i\omega_n) + \frac{w_1^{\uparrow} + w_1^{\downarrow}}{[G_{\sigma}^0(i\omega_n)]^{-1} - U}, \quad (5)$$

where $w_0 = 1 - w_1^{\uparrow} - w_1^{\downarrow}$ and w_1^{σ} are the localized electron occupancies for no f-electrons (w_0) and an f-electron with spin σ (w_1^{σ}); and finally (iii) the self-energy is determined by subtracting off the “bare” Green's function

$$\Sigma_{n\sigma} = [G_{\sigma}^0(i\omega_n)]^{-1} - G_{n\sigma}^{-1}. \quad (6)$$

The f-electron occupancies are found by explicitly calculating the path-integral for the partition function¹⁵ (generalized to include the magnetic field) and are determined by $w_0 = \mathcal{Z}_0/\mathcal{Z}$, $w_1^{\sigma} = \mathcal{Z}_1^{\sigma}/\mathcal{Z}$, and $\mathcal{Z} = \mathcal{Z}_0 + \mathcal{Z}_1^{\uparrow} + \mathcal{Z}_1^{\downarrow}$, with

$$\begin{aligned} \mathcal{Z}_0 &= \prod_{n=-\infty}^{\infty} Z_n^{\uparrow} Z_n^{\downarrow}, \\ \mathcal{Z}_1^{\sigma} &= \exp[-\beta(E_f + U - \mu - \frac{1}{2}g\mu_B\sigma h)] \prod_{n=-\infty}^{\infty} (Z_n^{\uparrow} - U)(Z_n^{\downarrow} - U), \end{aligned} \quad (7)$$

where $Z_n^{\sigma} := [G_{\sigma}^0(i\omega_n)]^{-1}$.

The algorithm for finding the self-consistent solution to these equations is the same as was used in the Hubbard model¹⁶: (i) begin with the self energy set equal to zero; determine the local Green's function from Eq. (3); (iii) determine the site-excluded Green's function from Eq. (4) and the f-electron occupancies from Eq. (7); (iv) determine the new local Green's function from Eq. (5) and the new self energy from Eq. (6). This new self energy is plugged back into step (ii) and the process is iterated until it converges (which typically takes less than 100 iterations for convergence to one part in 10^6).

In addition to finding the Green's functions in a magnetic field, we can also determine the susceptibilities to both charge-density-wave order and spin-density-wave order in zero magnetic field. The derivation of these quantities is similar to that of Brandt and Mielsch¹⁵, and we simply include details not presented before and summarize the generalizations needed when the electrons have spin.

We begin by adding an ordering field $\sum_j h_j^{\sigma} d_{j\sigma}^{\dagger} d_{j\sigma}$ to the Hamiltonian and examining the linear response in the limit as $h_j^{\sigma} \rightarrow 0$. The real-space conduction-electron correlation functions can be expressed in terms of the Green's functions via

$$\langle\langle n_{i\sigma}^d - \langle n_{i\sigma}^d \rangle \rangle \rangle \langle\langle n_{j\sigma'}^d - \langle n_{j\sigma'}^d \rangle \rangle \rangle = -T^2 \sum_n \frac{dG_{n\sigma}^{ii}}{dh_j^{\sigma'}}. \quad (8)$$

Following the standard techniques,¹⁵ one can express the correlation functions in terms of charge-density-wave (CDW) ($\tilde{\chi}$) and spin-density-wave (SDW) (χ) susceptibilities in momentum space

$$\begin{aligned}
\tilde{\chi}_n^{dd}(q) &= \chi_n^{dd0}(q) - T \sum_m \chi_n^{dd0}(q) \tilde{\Gamma}_{nm}^{dd} \tilde{\chi}_m^{dd}(q), \\
\chi_n^{dd}(q) &= \chi_n^{dd0}(q) - T \sum_m \chi_n^{dd0}(q) \Gamma_{nm}^{dd} \chi_m^{dd}(q),
\end{aligned} \tag{9}$$

where the susceptibility is found by summing over Matsubara frequencies [$\chi^{dd}(q) = T \sum_n \chi_n^{dd}(q)$], $\chi_n^{dd0}(q)$ is the bare particle-hole susceptibility,

$$\begin{aligned}
\chi_n^{dd0}(q) &= -T \sum_k G_n(k+q) G_n(k), \\
&= - \int_{-\infty}^{\infty} dy \frac{\rho(y)}{i\omega_n + \mu - \Sigma_n - y} \int_{-\infty}^{\infty} dz \frac{\rho(z)}{i\omega_n + \mu - \Sigma_n - X(q)y - z\sqrt{1 - X^2(q)}},
\end{aligned} \tag{10}$$

where all of the wavevector dependence is included in the term $X(q) = \sum_{j=1}^d (\cos q_j)/d$ (the Green's function and self energy in zero magnetic field have no spin dependence), and $\tilde{\Gamma}_{nm}^{dd}$ (Γ_{nm}^{dd}) are the irreducible CDW (SDW) vertex functions,

$$\tilde{\Gamma}_{nm}^{dd} =: \frac{1}{T} \left[\frac{d\Sigma_{n\uparrow}}{dG_{m\uparrow}} + \frac{d\Sigma_{n\uparrow}}{dG_{m\downarrow}} \right], \quad \Gamma_{nm}^{dd} =: \frac{1}{T} \left[\frac{d\Sigma_{n\uparrow}}{dG_{m\uparrow}} - \frac{d\Sigma_{n\uparrow}}{dG_{m\downarrow}} \right]. \tag{11}$$

Now the self energy can be expressed as an explicit function of the Green's function (of the same Matsubara frequency) and the f-electron filling [by substituting Eq. (4) into Eq. (5) and solving the resulting quadratic equation for Σ_n]

$$\Sigma_{n\sigma} = -\frac{1}{2G_{n\sigma}} + \frac{U}{2} \pm \frac{1}{2G_{n\sigma}} \sqrt{1 - 2(1 - 2w_1)UG_{n\sigma} + U^2G_{n\sigma}^2}, \tag{12}$$

with $w_1 = w_1^\uparrow + w_1^\downarrow$ the total f-electron concentration. The difficulty in calculating the derivatives (to find the irreducible vertices) arises from the fact that the f-electron filling w_1 is an explicit function of all of the Green's functions.

The CDW vertex becomes

$$\tilde{\Gamma}_{nm}^{dd} = \frac{1}{T} \left(\frac{\partial \Sigma_{n\uparrow}}{\partial G_{n\uparrow}} \right)_{w_1} \delta_{mn} + \frac{1}{T} \left(\frac{\partial \Sigma_{n\uparrow}}{\partial w_1} \right)_{G_{n\uparrow}} \left[\frac{\partial w_1}{\partial G_{m\uparrow}} + \frac{\partial w_1}{\partial G_{m\downarrow}} \right]. \tag{13}$$

In the zero-magnetic-field case, the two derivatives in the square brackets are equal to each other, which simplifies the analysis. Substituting into the Dyson equation Eq. (9) then yields

$$\tilde{\chi}_n^{dd}(q) = \chi_n^{dd0}(q) \frac{1 - \left(\frac{\partial \Sigma_{n\uparrow}}{\partial w_1} \right)_{G_{n\uparrow}} \gamma(q)}{1 + \chi_n^{dd0}(q) \left(\frac{\partial \Sigma_{n\uparrow}}{\partial G_{n\uparrow}} \right)_{w_1}}, \tag{14}$$

with the function $\gamma(q)$ defined by

$$\gamma(q) =: \sum_n \tilde{\chi}_n^{dd}(q) \left[\frac{\partial w_1}{\partial G_{m\uparrow}} + \frac{\partial w_1}{\partial G_{m\downarrow}} \right]. \tag{15}$$

Multiplying Eq. (14) by $\partial w_1/\partial G_{n\uparrow} + \partial w_1/\partial G_{n\downarrow}$ and summing over n yields an equation for $\gamma(q)$. Brandt and Mielsch show how to massage that formula into a form where the individual

derivatives can be explicitly calculated. The algebra is somewhat long, and entirely contained in their work. The final result for $\gamma(q)$ is

$$\gamma(q) = \frac{\sum_n \frac{\left(\frac{\partial w_1}{\partial Z_{n\uparrow}} + \frac{\partial w_1}{\partial Z_{n\downarrow}}\right) \left[1 - G_n^2 \left(\frac{\partial \Sigma_n}{\partial G_n}\right)_{w_1}\right]}{1 + G_n \eta_n(q) - G_n^2 \left(\frac{\partial \Sigma_n}{\partial G_n}\right)_{w_1}}}{1 - \sum_n \frac{G_n \eta_n(q) \left(\frac{\partial \Sigma_n}{\partial w_1}\right)_{G_n} \left(\frac{\partial w_1}{\partial Z_{n\uparrow}} + \frac{\partial w_1}{\partial Z_{n\downarrow}}\right)}{1 + G_n \eta_n(q) - G_n^2 \left(\frac{\partial \Sigma_n}{\partial G_n}\right)_{w_1}}}, \quad (16)$$

with $\eta(q)$ defined by

$$\eta_n(q) =: G_n \left[-\frac{1}{G_n^2} - \frac{1}{\chi_n^{dd}(q)} \right]. \quad (17)$$

Finally, the CDW susceptibility is computed from

$$\tilde{\chi}^{dd}(q) = -T \sum_n \frac{[1 - \gamma(q) \left(\frac{\partial \Sigma_n}{\partial w_1}\right)_{G_n}] G_n^2}{1 + G_n \eta_n(q) - G_n^2 \left(\frac{\partial \Sigma_n}{\partial G_n}\right)_{w_1}}. \quad (18)$$

This susceptibility diverges when $\gamma(q)$ diverges, which occurs when the denominator of Eq. (16) vanishes. This yields the same result as Brandt and Mielsch for the spinless case, except for an additional factor of 2 multiplying the sums in the numerator and the denominator arising from the two derivatives of w_1 (which are both equal).

Each of the derivatives appearing in Eqs. (16) and (18) can be directly calculated. A straightforward differentiation and simplification [employing the quadratic equation whose solution gave Eq. (12)] yields

$$\left(\frac{\partial w_1}{\partial Z_{n\uparrow}} + \frac{\partial w_1}{\partial Z_{n\downarrow}}\right) = \frac{2w_1(1-w_1)UG_n^2}{(1+G_n\Sigma_n)(1+G_n[\Sigma_n-U])}, \quad (19)$$

$$1 - G_n^2 \left(\frac{\partial \Sigma_n}{\partial G_n}\right)_{w_1} = \frac{(1+G_n\Sigma_n)(1+G_n[\Sigma_n-U])}{1+G_n(2\Sigma_n-U)}, \quad (20)$$

and

$$G_n^2 \left(\frac{\partial \Sigma_n}{\partial w_1}\right)_{G_n} = \frac{UG_n^2}{1+G_n(2\Sigma_n-U)}. \quad (21)$$

For the cases examined here, we never found any divergences of the CDW susceptibility.

We must follow a similar procedure to find the SDW susceptibility, but the algebra simplifies tremendously in zero external field, because the irreducible SDW vertex becomes

$$\Gamma_{nm}^{dd} = \frac{1}{T} \left(\frac{\partial \Sigma_{n\uparrow}}{\partial G_{n\uparrow}}\right)_{w_1} \delta_{mn}, \quad (22)$$

since the derivatives with respect to w_1 are equal and hence cancel. The SDW susceptibility then assumes the simple form

$$\chi^{dd}(q) = -T \sum_n \frac{G_n^2}{1 + G_n \eta_n(q) - G_n^2 \left(\frac{\partial \Sigma_n}{\partial G_n} \right)_{w_1}}, \quad (23)$$

which is never expected to diverge at any finite temperature.

Brandt and Mielsch also show how to calculate the mixed susceptibilities that correlate the d-electron charge (or spin) with the f-electron charge (or spin). The idea is that derivatives of w_{1i}^σ with respect to the ordering field h_j^σ produce the mixed susceptibilities, so a direct calculation of the dd -susceptibility involves total derivatives of the self energy with respect to the Green's functions, which can be expressed in terms of the irreducible vertex (as done above) to find the susceptibility, or can be expressed as partial derivatives with respect to the Green's function and the f -electron filling (since the self energy is a function of G_n and w_1). Hence one can solve directly for the mixed susceptibilities (the details appear in Brandt and Mielsch's work). The final result for the mixed CDW susceptibility is

$$\tilde{\chi}^{df}(q) = \frac{\left[1 + G_n \eta_n(q) - G_n^2 \left(\frac{\partial \Sigma_n}{\partial G_n} \right)_{w_1} \right] \tilde{\chi}_n^{dd}(q) + G_n^2}{G_n^2 \left(\frac{\partial \Sigma_n}{\partial w_1} \right)_{G_n}} = \gamma(q), \quad (24)$$

in which the Matsubara-frequency dependence actually drops out of the expression [after using Eq. (14)], and it is equal to $\gamma(q)$. Similarly, we find the mixed SDW susceptibility vanishes $\chi^{df}(q) = 0$.

Now, we could have also calculated the mixed susceptibility by adding an ordering field for the f -electrons, and differentiating the d -electron Green's function with respect to the f -electron ordering field. The results of each of these calculations must be the same, since the df -susceptibility is equal to the fd -susceptibility. However, if we write out the expression for the fd -susceptibility explicitly in terms of the derivatives with respect to the f -electron-ordering field, we find that it includes a dependence on the ff -susceptibility. Hence the ff -susceptibility can be determined from the df -susceptibility found above. In the CDW channel, one finds that the ff -susceptibility satisfies

$$\tilde{\chi}^{ff}(q) = \frac{1}{2T} \frac{\tilde{\chi}^{df}(q)}{\sum_n \frac{G_n^2 \left[\left(\frac{\partial \Sigma_n}{\partial w_{1\uparrow}} \right)_{G_n} + \left(\frac{\partial \Sigma_n}{\partial w_{1\downarrow}} \right)_{G_n} \right]}{1 + G_n \eta_n(q) - G_n^2 \left(\frac{\partial \Sigma_n}{\partial G_n} \right)_{w_1}}}. \quad (25)$$

This result can be further simplified following the same steps as above, to rewrite the derivatives in terms of explicitly calculable quantities. After a significant amount of algebra, similar to what was done for the dd -susceptibility in the CDW channel, we find

$$\tilde{\chi}^{ff}(q) = \frac{\frac{1}{T} w_1 (1 - w_1)}{1 - \sum_n \frac{G_n \eta_n(q) \left(\frac{\partial \Sigma_n}{\partial w_1} \right)_{G_n} \left(\frac{\partial w_1}{Z_{n\uparrow}} + \frac{\partial w_1}{Z_{n\downarrow}} \right)}{1 + G_n \eta_n(q) - G_n^2 \left(\frac{\partial \Sigma_n}{\partial G_n} \right)_{w_1}}}, \quad (26)$$

which has the same denominator as the dd - and df -susceptibilities. The CDW transition temperature, is thereby determined by the condition that this denominator vanishes.

A similar analysis for the SDW channel does not yield any useful information because $\chi^{df}(q) = 0$. Instead, we can directly compute the uniform ($q = 0$) ff -susceptibility for SDW

order by differentiating the fillings w_1^σ with respect to the f -levels E_f^σ . The calculation is simplified by the fact that the factors Z_n^σ depend only on the total f -electron filling w_1 which does not change in a magnetic field (only the relative fillings $w_1^\uparrow - w_1^\downarrow$ change), and the final result is

$$\chi^{ff}(0) = \frac{w_1}{2T}, \quad (27)$$

which is in the Curie-Weiss form.

III. RESULTS

We present the magnetic response of our numerical solutions for a variety of different cases in Figure 1. Each figure corresponds to a different value of total electron concentration ($n = n_d + n_f$), with ten values of E_f/t^* ranging from 0 to 4.5 in steps of 0.5. Fig. 1(a) is a typical high-density result. There are 2.5 electrons per impurity site, implying $n_f \neq 0$ at all temperatures, leading to a Curie contribution to the susceptibility at small T . In this regime, the results are rather insensitive to U and E_f ($U = 10t^*$ here). Fig. 1(b) is the $n = 2.1$ case. We chose $U = t^*$ here, and the results have a stronger dependence on E_f , showing a downturn at moderate T , before the Curie-law divergence sets in for $T \rightarrow 0$. Neither of these cases have a charge-transfer transition, rather they always display a Curie-like divergence as $T \rightarrow 0$. As n is decreased to 2 and beyond, it is no longer necessary for there to be any f electrons remaining at $T = 0$, and χ^{ff} can vanish in that limit. In Fig. 1(c) we plot χ^{ff} for $n = 2$ and $U = 2t^*$, showing an asymmetric peak that increases in size and sharpens as the turnover temperature T_V decreases, and which still has a weaker Curie upturn at the lowest temperatures, because $n_f \neq 0$ as $T \rightarrow 0$. Here, the results depend on E_f and U , with the peak lowering in magnitude and broadening as U increases, and the low-temperature upturn becoming more prominent. The case $n = 1.9$ is shown in Fig. 1(d) for $U = 10t^*$. Once again we have a dependence on E_f and U , but the low-temperature upturn has disappeared. In some cases χ^{ff} has a double-hump structure. Finally the low-density regime is plotted in Fig. 1(e) ($n = 0.5$, $U = 10t^*$). Here, as in the high-density limit, the results are insensitive to U . The reason why the results do not depend sensitively on U for both the high and low-density limits is that when n_f is small, then the Falicov-Kimball model looks like a noninteracting free band, because there are no localized electrons for the conduction electrons to scatter off of. Similarly, in the high density regime, as n_f approaches 1, the model also becomes noninteracting, since there is an f -electron at every site, and the conduction band is simply shifted in energy by U , which does not affect any of the qualitative physics.

The model also exhibits a metamagnetic transition, for large enough magnetic fields. This is shown in Figure 2 for one case: $n = 2$, $E_f = t^*$, $U = 2t^*$, $g = 4.5$, and eight temperatures from $0.05t^*$ up to $6.4t^*$. The numerical analysis shows that at $T = 0$, the Zeeman energy at the transition is of the order of $k_B T_V$. The metamagnetic field, H_V , decreases at higher temperatures but the transition becomes smoother. The metamagnetism disappears as T is increased beyond T_V , because the f -electrons are already occupied in the zero-field limit.

This anomalous behavior can be understood in terms of simple thermodynamic considerations. For $E_f > \mu$ and $n < 2$, the nonmagnetic empty f -orbital is energetically more

favorable than the magnetic state, so the ground state has no f -electrons. However, at high T , the large magnetic entropy of the f -electron spins favors the magnetic state. The susceptibility of these f -electrons grows rapidly as the temperature is reduced until, close to T_V , the entropy gain is insufficient to compensate the energy loss and the f -electrons disappear to form a nonmagnetic state. Thus, χ^{ff} drops rapidly, which is the origin of the sharp asymmetric peak in the $\chi(T)$ data.

IV. APPLICATION TO REAL MATERIALS

The insulating state of NiI_2 is best described by a hole picture. The localized holes lie in the Ni d -bands, and there is one hole per site. The Iodine p -band is full, so there are no conduction holes. Hence the total hole concentration is 1 and in the regime where the pressure is tuned to lie just above the metallization pressure at $T = 0$, we expect the susceptibility to look qualitatively like the low-density regime of Fig. 1(e) (this is because the only difference between the hole picture and the electron picture is that the f -level energy changes sign). So, we expect an interesting anomalous magnetic response of NiI_2 when the pressure is sufficiently high that the system is just on the metallic side of the metal-insulator transition point. In this case, there are few localized holes at low temperature, but they will be thermally excited in large numbers as the temperature is raised. The susceptibility should be quite small at low temperature, and then rise dramatically as the metal-insulator transition point is passed (before turning over again at higher temperature). Also, we predict that NiI_2 should exhibit metamagnetism. Since new techniques allow one to inductively measure the magnetic response of samples in a diamond-anvil cell,¹⁷ without the need of attaching any wires within the cell, it is possible that one could use this anomalous magnetic response to accurately measure the phase diagram of NiI_2 . To our knowledge no measurements of the magnetic response of NiI_2 under pressure have yet been carried out. Only the Néel temperature in the insulating phase was measured with the Mössbauer effect.²

For the Yb-based VF compounds, the mapping of this system to an effective Falicov-Kimball model is more complicated than in NiI_2 , and more controversial, so we begin by motivating how such a mapping can be made, and provide experimental evidence that supports this novel point of view. We notice first that there is no simple relation between the change in the lattice parameter (that is, the change in Yb-In hybridization) and the onset of the anomalies. In $\text{Yb}_{1-x}\text{Y}_x\text{InCu}_4$ an increase of $a(x)$ is accompanied by a decrease of T_V and H_V . In $\text{YbIn}_{1-x}\text{Ag}_x\text{Cu}_4$, $a(x)$ does not change when In ions are replaced by smaller Ag ions (for $x \leq 0.4$) while T_V and H_V increase and the anomalies become less sharp^{18,8}. In stoichiometric YbInCu_4 , T_V and H_V are enhanced by thermal treatment, which introduces disorder between Yb and In sites but does not change a (or the Yb-In hybridization). We notice also that systems which are similar for $T \gg T_V$ ($H \gg H_V$) and $T \ll T_V$ ($H \ll H_V$) can show substantial variation in the onset and the shape of the anomalies at T_V and H_V . To account for such a behavior we assume that the effective f -state is in the proximity of the chemical potential, μ , so that correctly placed Yb ions are in the VF state. Hence, the important parameter is the renormalized position of the f -level, $E_f - \mu$, which provides the characteristic energy scale (typically, about 100 K).

The assumption that the majority of Yb ions are in the VF state for $T \gg T_V$ is supported by the unusual deviation from Vegard's law found in $\text{YbIn}_{1-x}\text{Ag}_x\text{Cu}_4$ for $x \leq 0.4$ at room

temperature.⁸ Here, the replacement of In ions by smaller Ag ions does not modify $a(x)$, since in a VF compound the Yb ions reduce their average valence and preserve the volume of the unit cell. The assumption that $E_f - \mu$ increases only slightly with x , explains the weak concentration dependence of the high-temperature susceptibility and the high-field saturation magnetization^{18,8}. For $x \leq 0.4$, E_f is pushed off μ , which results in a HF compound with a stable f-shell.^{18,8}

To explain the anomalies at T_V , we assume that the magnetic response of these Yb compounds has its origin in two physically distinct components. The first one, χ_{VF} , is due to the hybridized (correctly placed) Yb ions, and is large (on an absolute scale), isotropic, and sample independent. The second component of the susceptibility, χ^{ff} , arises from the unhybridized Yb ions which switch at T_V (or H_V) from the magnetic 3+ to the nonmagnetic 2+ configuration. Hence, χ^{ff} vanishes below T_V and is smaller than χ_{VF} at high temperatures, but dominates $\chi(T)$ near T_V ; it is strongly sample dependent. At low temperatures and high fields these unhybridized states lead to a metamagnetic transition with a small energy difference between the low-field and the high-field states.

The lattice of YbInCu₄ unit cells separates into two distinct sublattices: the sublattice of unhybridized Yb ions (localized f-electrons) and the sublattice of hybridized Yb ions. Conduction electrons from the In ions move (via nearest-neighbor hopping between unit cells of the full lattice) between any two unit cells of the unhybridized-Yb-ion sublattice. Hence, if we focus only on the sublattice degrees of freedom, we can model the d-band by a *single effective band* that couples any two sites of the sublattice with a *random* hopping matrix element (that depends on the growth and thermal treatment of the sample). These f and d states have a common chemical potential (μ) and interact by a Coulomb repulsion (U) when they occupy the same unit cell. In addition, both the d and f particles carry a spin label σ and the d -level can accommodate 2 electrons (or holes) of the opposite spin. The occupancy of the f -level is restricted to $n_f \leq 1$ because of the large Coulomb repulsion ($U_{ff} \sim \infty$) of the f -particles of opposite spins. To discuss the Yb-based VF compounds we use the hole-picture, in which $E_f < \mu$ and the total number of holes at the ill-placed sites is restricted to $n_h = n_d^h + n_f^h \leq 3$. (In the electron-picture, one would have $E_f > \mu$ and would restrict the total number of electrons to $n_e = n_d^e + n_f^e \leq 3$.) The magnetic field h couples to the f and d states but with different g -factors ($g = 4.5$ for the f -holes). This picture is thus described by the spin one-half Falicov-Kimball model. In the limit $N \rightarrow \infty$ ²¹, and $N/N_l \ll 1$, our choice for t_{ij} maps this problem onto the infinite-dimensional (local) one, which allows the magnetic susceptibility to be evaluated exactly using the methods described above.

The hole filling for these Yb-based VF compounds lies near $n \approx 2$. The exact solution reproduces well the overall behavior of the experimental data. Figs.(1c)-(1d) capture most of the features shown^{3-5,8} by $\chi(T)$, such as an asymmetric peak at T_V that increases in magnitude and sharpens as $T_V \rightarrow 0$, while Fig.(2) explains the magnetization^{4,11} $M(T)$, with a metamagnetic transition that smoothes out and then disappears as T is increased. Various samples will have different numbers of Yb impurities and will require different values of t^* , E_f , and n^h . Our analysis shows that the lower the transition temperature, the more pronounced and steeper the anomaly. For large fields, unhybridized Yb ions switch to a magnetic configuration at much lower temperatures, than in the absence of the field.

We emphasize that in the model proposed here, most of the Yb ions are in a hybridized

(VF) state at all temperatures and that the anomalies around T_V are *due to an entropy driven transition of a small number of unhybridized Yb ions*, so that the bulk of the lattice is unchanged at T_V . On the other hand, in the commonly used hybridization model it is assumed that all the Yb ions switch at T_V from a stable 3+ configuration to a hybridized VF configuration, which makes the high-T and the low-T phases fundamentally different. Thus, the appropriate model for describing the Yb-based VF compounds can be determined by measuring the pressure dependence of $\Delta a/a$ across T_V . The Falicov-Kimball model predicts a weak pressure dependence because the ions involved in the transition are unhybridized, while the hybridization model predicts a strong pressure dependence because the hybridization rapidly increases with pressure.

V. CONCLUSIONS

In summary, we have exactly solved the spin-one-half Falicov-Kimball model on an infinite-dimensional hypercubic lattice in an external magnetic field. We also examined the magnetic response (as a function of temperature) in zero magnetic field. The system showed anomalous behavior due to the proximity of the f -electron states (which have local moments) to the chemical potential, which allows their occupancy to change dramatically as the temperature changes, because of the entropy gain due to the magnetic moments. Thus, the uniform magnetic susceptibility shows an asymmetric peak at a characteristic temperature T_V , which decays like a Curie-Weiss law for high temperatures (because of the f -moments) and typically decays exponentially rapidly for temperatures much lower than T_V (because the f -electrons are thermally excited across a gap). The magnetization (in an external magnetic field) shows metamagnetic behavior because of the rapid switching of electrons from the d - to the f -states when $T < T_V$, but shows a much smoother increase with magnetic field for temperatures larger than T_V .

We applied this model to two candidate real materials. The first is NiI_2 , which is known to undergo a charge-transfer metal-insulator transition as a function of pressure, that is well described by the Falicov-Kimball model. We propose that the metal-insulator phase diagram, and this anomalous magnetic behavior can be easily measured using newly developed techniques within a diamond-anvil cell. The second are the Yb-based VF compounds whose anomalous magnetic properties can be attributed to an entropy-driven transition of disordered Yb and explained by the Falicov-Kimball model with random hopping. The Falicov-Kimball-transition of unhybridized Yb ions and the VF behavior of hybridized Yb ions are both due to the proximity of the f -level to the chemical potential. The two inequivalent Yb sites appear in these compounds because of their characteristic crystal structure. Thus, the large changes in magnetic, transport, and elastic properties at T_V and H_V are explained, and reconciled with small changes in the f -electron valence and Δa . This proposed alternative explanation for the magnetic response of the Yb-based VF compounds is controversial, and differs from the more conventional description (which does not have any quantitative theoretical description). We propose high-pressure experiments to differentiate between the two proposed theories.

ACKNOWLEDGMENTS

We acknowledge useful conversations with I. Aviani, Z. Fisk, M. Jarrell, B. Lüthi, M. Miljak, and J. Sarrao. J. K. F. acknowledges the Donors of The Petroleum Research Fund, administered by the American Chemical Society, for partial support of the early stages of this research (ACS-PRF No. 29623-GB6) and the Office of Naval Research Young Investigator Program (N000149610828) for supporting the later stages of this work. The early stages of this project have also been funded in part by the National Research Council under the Collaboration in Basic Science and Engineering Program. The contents of this publication do not necessarily reflect the views or policies of the NRC, nor does mention of trade names, commercial products, or organizations imply endorsement by the NRC.

[†] Permanent address: Institute of Physics, Zagreb, Croatia.

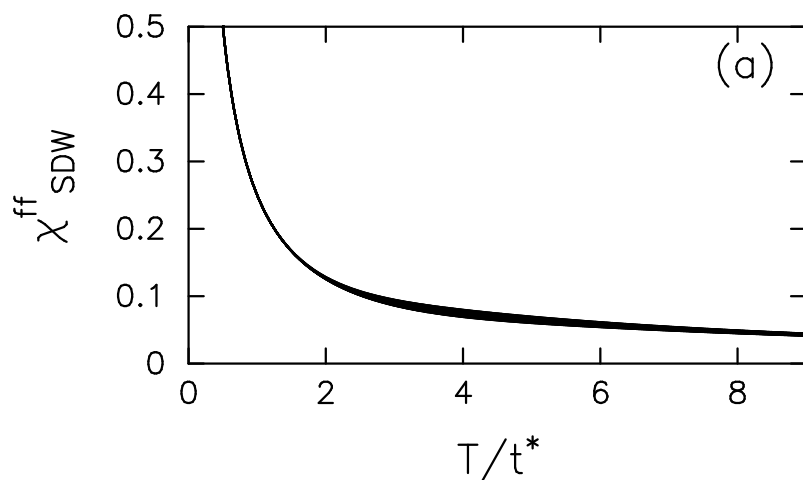
REFERENCES

- ¹ L. M. Falicov and J. C. Kimball, Phys. Rev. Lett. **22**, 997 (1969); R. Ramirez, L. M. Falicov and J. C. Kimball, Phys. Rev. B **2**, 3383 (1970).
- ² M. P. Pasternak, R. D. Taylor, A. Chen, C. Meade, L. M. Falicov, A. Giesekus, R. Jeanloz, and P. Y. Yu, Phys. Rev. Lett. **65**, 790 (1990); J. K. Freericks and L. M. Falicov, Phys. Rev. **45**, 1896 (1992); A. L. Chen, P. Y. Yu, and R. D. Taylor, Phys. Rev. Lett. **71**, 4011 (1993).
- ³ I. Felner and I. Novik., Phys. Rev. B **33**, 617 (1986); I. Felner, et al., Phys. Rev. B **35**, 6956 (1987).
- ⁴ K. Yoshimura, et al., Phys. Rev. Lett. **60**, 851 (1988); T. Shimizu et al., J. Phys. Soc. Japan **57**, 405 (1988).
- ⁵ B. Kindler, et al., Phys. Rev. B **50**, 704 (1994).
- ⁶ K. Kojima, et al., J. Phys. Soc. Japan, **59**, 792 (1990).
- ⁷ H. Nakamura, et al., J. Phys. Soc. Japan **59**, 28 (1990).
- ⁸ J.L. Sarrao et al., Physics B, **223&224**, 366 (1996).
- ⁹ H. Junhui, et al., J. Phys. Soc. Japan, **66**, 2481 (1997).
- ¹⁰ J. M. Lawrence et al., Phys. Rev. B **54**, 6011 (1996).
- ¹¹ H.A. Katori, et al., Physica B, **201**, 159 (1994).
- ¹² T. Portengen, T. Ostreich, and L. J. Sham, Phys. Rev. B **54**, 17452 (1996); Phys. Rev. Lett. **76**, 3384 (1996).
- ¹³ P. Farkašovský, Phys. Rev. B **51**, 1507 (1995); **52**, R5463 (1995); **54**, 11261 (1996); Z. Phys. B **104**, 147 (1997); **104** 553 (1997); M. Park and J. Hong, unpublished.
- ¹⁴ W. Metzner and D. Vollhardt, Phys. Rev. Lett. **62**, 324 (1989).
- ¹⁵ U. Brandt and C. Mielsch, Z. Phys. B **75**, 365 (1989); Z.Phys. B **79**, 295 (1990); U. Brandt, A Fledderjohann, and G. Hülsenbeck, Z. Phys. B **81**, 409 (1990); U. Brandt and A. Fledderjohann, Z. Phys. B **87**, 111 (1992).
- ¹⁶ M. Jarrell, Phys. Rev. Lett. **69**, 168 (1992).
- ¹⁷ V. V. Struzhkin, Y. A. Timofeev, R. J. Hemley, and H.-K. Mao, Phys. Rev. Lett. **79**, 4262 (1997).
- ¹⁸ K. Yoshimura et al., J. Mag. Mag. Mat. **90&91**, 466 (1990).
- ¹⁹ N. Pillmayr et al., J. Mag. Mag. Mat. **104&107**, 639 (1992).
- ²⁰ We choose a Gaussian density of states rather than Wigner's semicircular density of states in order to include the effects of Lifshitz's tails. The theory is rather insensitive to the precise choice of $\rho(\epsilon)$. For details on this choice, see M. Moshe, H. Neuberger, and B. Shapiro, Phys. Rev. Lett. **73**, 1497 (1994); M. Kreynin and B. Shapiro, Phys. Rev. Lett. **74**, 4122 (1995).
- ²¹ M. J. Rozenberg et al., Phys. Rev. B **49**, 10181 (1994).

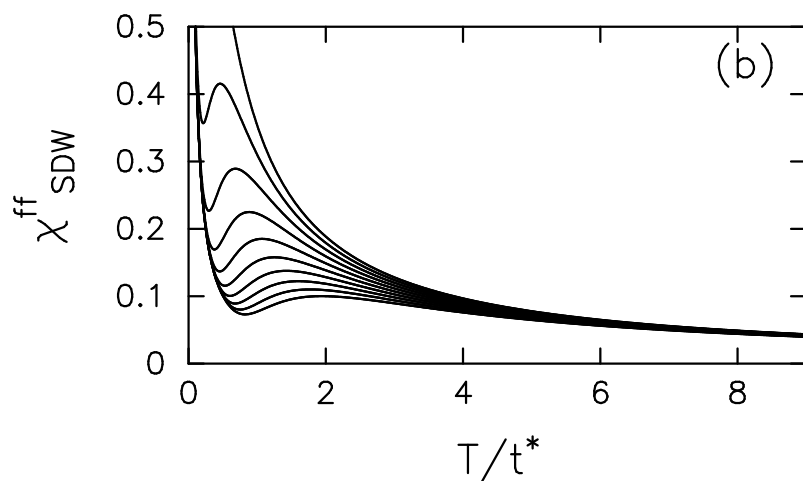
FIGURES

FIG. 1. Magnetic susceptibility of the f -electrons in the Falicov-Kimball model. The different curves correspond to $E_f/t^* = 0.0, 0.5, \dots, 4.5$ (in general E_f increases from top to bottom in these figures). The different figures are: (a) $n = 2.5$ and $U = 10t^*$; (b) $n = 2.1$ and $U = t^*$; (c) $n = 2.0$ and $U = 2t^*$; (d) $n = 1.9$ and $U = 10t^*$; and (e) $n = 0.5$ and $U = 10t^*$.

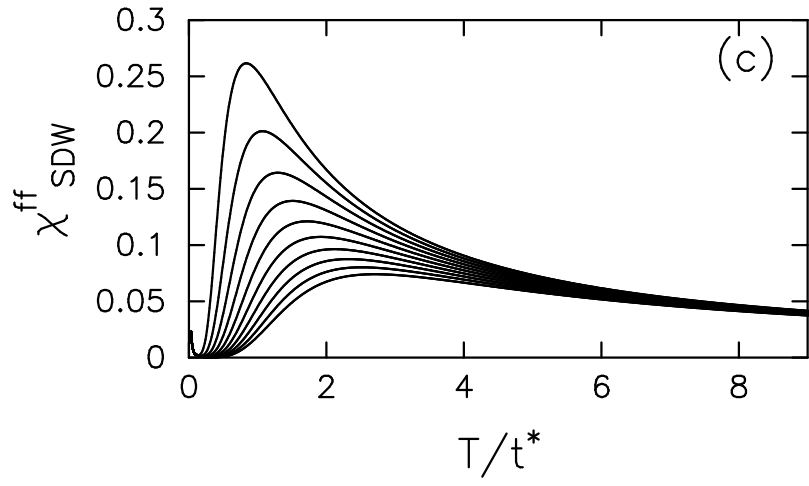
FIG. 2. Total magnetization of the Falicov-Kimball model as a function of magnetic field. The different curves correspond to different temperatures: $T/t^* = 0.05, 0.1, 0.2, \dots, 3.2, 6.4$ (the temperature increases from top to bottom in the large- h range). The parameters are $n = 2$, $E_f = t^*$, and $U = 2t^*$.



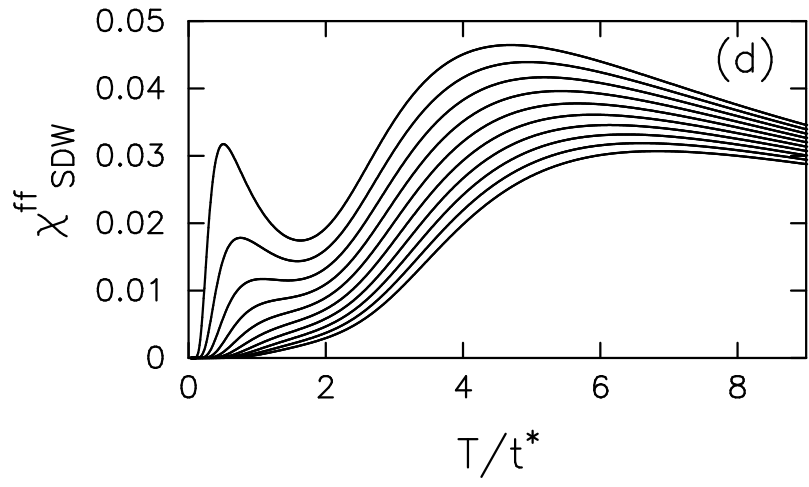
Freericks and Zlatic, Phys. Rev. B, Figure 1(a)



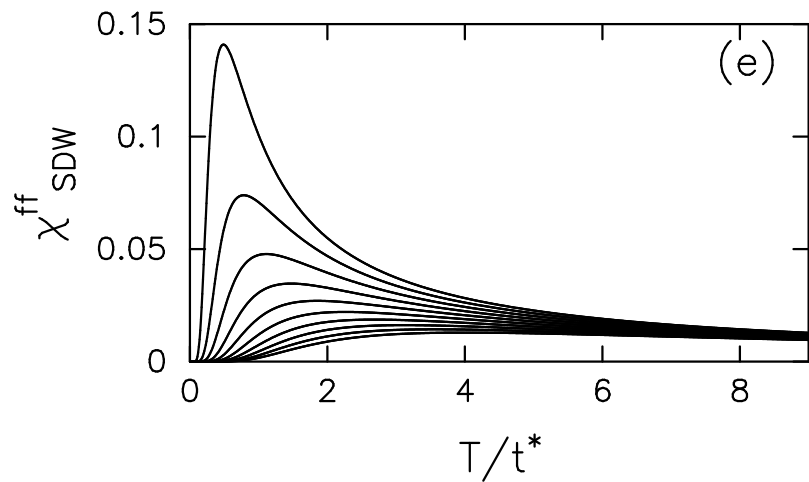
Freericks and Zlatic, Phys. Rev. B, Figure 1(b)



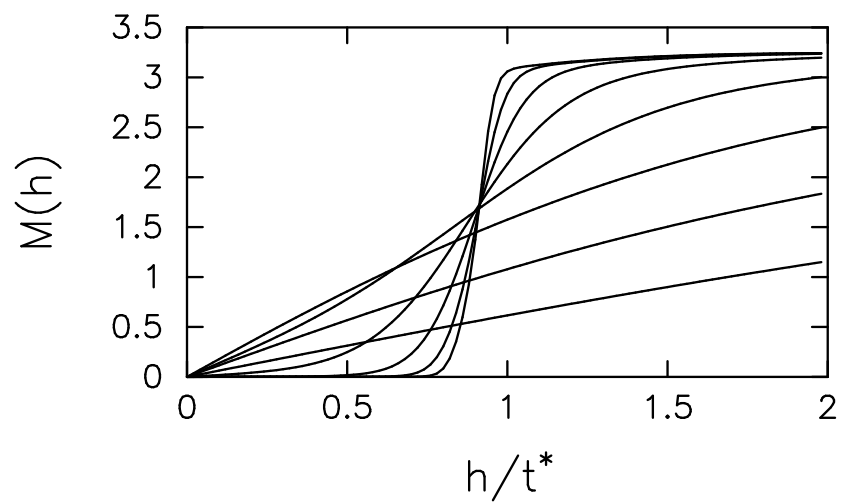
Freericks and Zlatic, Phys. Rev. B, Figure 1(c)



Freericks and Zlatic, Phys. Rev. B, Figure 1(d)



Freericks and Zlatic, Phys. Rev. B, Figure 1(e)



Freericks and Zlatic, Phys. Rev. B, Figure 2